Conformational Analysis of 2,2′-Bithiophene: A ^{1}H Liquid Crystal NMR Study Using the ^{13}C Satellite Spectra

Maria Concistré,[†] Luana De Lorenzo,[†] Giuseppina De Luca,[†] Marcello Longeri,*[,†] Giuseppe Pileio,[†] and Guido Raos[‡]

Dipartimento di Chimica, Universitá della Calabria, Via P. Bucci, 87030 Arcavacata di Rende (Cs), Italy, and Dipartimento di Chimica, Materiali e Ingegneria Chimica, Politecnico di Milano, I-20131 Milano, Italy

Received: July 20, 2005; In Final Form: September 14, 2005

We have obtained a very large data set of spectral parameters from the analysis of ^{1}H NMR and ^{13}C satellite spectra of 2,2′-bithiophene dissolved in anisotropic, partially orienting mesophases. In particular, this parameter set includes 33 dipolar couplings, which are directly related to the interatomic distances, the dihedral angle ϕ between the two thiophenic rings, and the anisotropic solute−solvent interaction potential. This allows an exhaustive investigation of the conformational equilibrium of 2,2′-bithiophene in a liquidlike phase. Comparison with the predictions of high-level theoretical calculations for the isolated molecule provides evidence of a strong flattening as well as the sharpening effect of the medium on the conformer population. The approximations needed to apply vibrational corrections to flexible molecules are discussed in detail and some general conclusions concerning their effect on structure and conformational equilibria are proposed.

1. Introduction

α-Conjugated oligo- and polythiophenes display peculiar electrical and optical properties, making them ideal candidates for a number of organic-based electronic and optoelectronic applications.[1−3] Their semiconductivity and luminescence depend critically on the intramolecular delocalization of the π electrons along the conjugated chain and, as a consequence, on the extent of the overlap between the p_z orbitals of the carbon atoms in the α−α′ positions.[4,5] The torsion potential around the α−α′ bonds also affects the ability of the molecules to assemble in the solid state,[6] and its proper inclusion has been found to be crucial for realistic molecular modeling studies.[7]

The determination of the conformational equilibrium is thus very important and the simplest compound of the series, 2,2′-bithiophene, has been investigated in the past by computational approaches (see, for example, refs 4, 8, and 9 and reference therein) and by many different experimental techniques in (i) gas phase (electron diffraction[10,11] and fluorescence[12,13]), (ii) solid state (X-ray diffraction[14]), and (iii) liquid phase (dipole moment,[15] Kerr constant,[16] photoelectron[17] and UV[18,19] spectroscopies). Unfortunately, the quantitative evaluation of the internal rotation potential poses particularly difficult problems from the experimental side.[20,21] At the same time, the outcome of ab initio theoretical calculations are strongly dependent on the computational approach (i.e., SCF, MP2 or DFT variants, the base dimension being a critical issue[9]).

The potentialities of liquid crystal NMR spectroscopy (LX-NMR) in investigating conformational equilibria in liquid phases are well-known.[22−24] Such potentialities are enhanced in the case of single rotors composed of two rigid aromatic moieties linked by a single bond.[21] In fact, thanks to the validity of the rigid rotor hypothesis and the intrinsically simple (by symmetry) rotation potential function, it has been possible to determine with good accuracy the position of the internal potential minima of biphenyl,[25] and in addition, to test the reliability of different models proposed to decouple internally from overall molecular rotation.

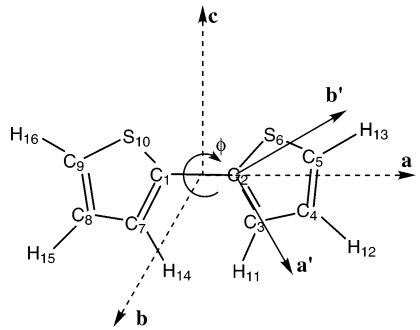

Figure 1. Structure and atomic labeling for 2,2′-bithiophene. Reference axes for the whole molecule (---) and the ring fragment (—). The latter lies on the *a*′*b*′ plane with the axes *c*′ orthogonal. ϕ is the S−C−C−S torsion angle, equal to 0° for the syn-planar conformer and to 180° for the trans-planar conformer. The dihedral angle between the ring planes is equal to $\phi^{syn} = \phi$ for $0° \le \phi \le 90°$ and to $\phi^{anti} = 180° - \phi$ for $90° \le \phi \le 180°$.

Compared to biphenyl, determination of the conformational equilibrium of 2,2′-bithiophene (and its bifuryl homologue[26]) represents a more challenging problem. Although the rigid rotor hypothesis is still valid, the internal rotation function is more complex because there are distinct pairs of symmetry-related syn-gauche and anti-gauche conformers (which could degenerate in a syn-planar and anti-planar form). Henceforth, we use ϕ to denote the S−C−C−S torsion angle ($0° \le \phi \le 180°$) and we use either ϕ^{syn} or ϕ^{anti} to denote the dihedral angle between the planes of the aromatic rings. These are related by $\phi^{syn} = \phi$ for $0° \le \phi \le 90°$ and $\phi^{anti} = 180° - \phi$ for $90° \le \phi \le 180°$ (see Figure 1).

Within the rotational isomeric state (RIS) hypothesis adopted by Ter Beek et al.,[27] the best fit between calculated and experimental D_{HH} couplings (the only available at the time) was found for $\phi^{syn}_{min} = 24°$ and a syn-gauche population $p^{syn} \cong 30\%$, hav-

* Corresponding author. Fax (+39) 0984 493301, E-mail: m.longeri@unical.it.
[†] Universitá della Calabria.
[‡] Politecnico di Milano.

10.1021/jp054003f CCC: $30.25 © 2005 American Chemical Society
Published on Web 10/19/2005

ing assumed, among other things, $\phi_{min}^{anti} = 0°$. However, different outcomes are also reported in the literature.[28,29] Quite simply, there are not enough data (three intra-ring plus six conformationally dependent inter-ring D_{HH}'s) for an unbiased determination of the conformational equilibrium. Remembering that (i) D_{ij} show a strong dependence on internuclear distances, (ii) not all dipolar couplings may be strongly dependent on the internal rotation angle, and (iii) no direct information on the molecule carbon structure is available from the analysis of ^{1}H anisotropic spectra, it is not surprising that different conformational hypotheses and/or models to decouple internal from overall rotation motions will fit the D_{ij} data set, producing "reasonable" but slightly different sets of inter-protonic distances.[21]

Such difficulties could be eliminated if an oversized data set and a strong "geometry based" filter were available, as from the analysis of ^{1}H spectra of selectively ^{13}C-enriched isotopomers or, better, of satellite spectra of "dilute" nuclei (typically ^{13}C nuclei). In this way it was possible (i) to accomplish very precise structural determinations of small, highly symmetric "rigid" molecules,[30] i.e., molecules displaying only small amplitude vibrational motion, and (ii) to demonstrate that the "solvent induced distortion effects" are a consequence of having neglected the coupling between molecular vibrations and overall orientation motions.[31,32]

There are two major obstacles that have limited this approach to a very few cases. The first, shared by both rigid and flexible molecules, follows from the difficulties in recognizing and assigning weak satellite transitions in the presence of the much more intense lines belonging to the all-^{12}C isotopomer: only those few not hidden under the ^{1}H transitions or lost in the signal noise would be observed and assigned. As a consequence, errors in the spectral analysis of satellite spectra cannot be ruled out and a lower precision of the dipolar couplings to "dilute" nuclei is expected. A recently proposed approach,[33,34] giving satellite spectra separated from one another by an HSQC experiment, seems very promising and could overcome these problems. The second problem, specific of flexible molecules, is related to the way the vibrational correction procedure has to be applied in the presence of large amplitude motions. Because such corrections can be as high as 10% on $^1D_{HC}$,[30,35] its proper application is very important if correct molecular geometries are to be obtained. Some of the still open questions and the effects of the proposed approximations will be discussed in detail in the following sections.

If the full set of D_{HC} couplings were available from the analysis of ^{13}C satellite spectra, for 2,2′-bithiophene there would be a total of 33 D_{ij}'s−15 fixing the structure of the thiophene ring and 18 depending on ϕ and on $r_{C_1C_2}$ (see Figure 1). The problem would be well overdetermined and a more conclusive answer to the conformational problem can be expected. The decoupling of internal and overall rotation motions will be carried out using the additive potential (AP) model.[22,23,36] Rather than describing the potential energy function, a novel approach[37] that gives a direct probability description of the conformational distribution will be used.

2. Experimental Procedures and Methods

Two solutions, both approximately 10 wt %, were prepared by dissolving 2,2′-bithiophene (by Aldrich, used without further purification) in I52 (IH) and ZLI1132 (IIH) (from Merck Darmstadt), two nematic liquid crystals (LC) of positive magnetic anisotropy. Their chemical structures are reported in Figure 2.

The samples were heated a few times up to their clearing points, strongly shaken to give very homogeneous solutions,

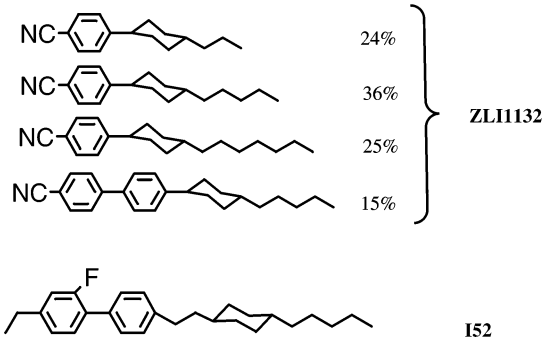

Figure 2. Structure and composition for the liquid crystals ZLI1132 and I52.

and left to cool slowly in the magnet. The spectra were recorded at room temperature on a Bruker AMX600 working at 14.09 T, averaging over 4000 free induction decays to obtain a high S/N ratio. With an experimental spectral width of 14 kHz, a 64K points FID gave a digital resolution of 0.3 Hz/point.

The ^{13}C, ^{1}H coupled, spectra of 2,2′-bithiophene in $CDCl_3$ were recorded on a Bruker Advance300 working at 7.04 T with a 0.03 Hz/point digital resolution. The $^nJ_{C_kH}$ values ($k = 3-5$) were determined by inspection and assigned according to literature.[38] For $k = 2$, the nearly first order, 2^6 lines, dddddd $^{13}C_2$ spectrum was analyzed using as the starting set the indirect couplings determined by inspection of the $\{^1H\}-^{13}C_2$ selectively decoupled spectra. The J_{ij} values are reported in Table 1. Signs of $^3J_{C_2H_{15}}$, $^4J_{C_2H_{14}}$, and $^5J_{C_2H_{16}}$ and the assignment of the two latter couplings, were assumed by comparison with previous experiments.

2.1. Spectral Analysis. The ^{1}H spectrum is made by transitions due to four AA′BB′CC′X spin systems (neglecting isotopic effect on chemical shifts), dispersed underneath the much more intense lines due to the AA′BB′CC′ isotopomer. Therefore great care has to be taken during spectral analysis to avoid false solutions and produce unquestionable spectral parameters. As a first step, the ^{1}H spectrum of AA′BB′CC′ was analyzed using a graphic interactive procedure (dubbed ARCANA) developed from ref 39, using the D_{HH} values from ref 27 as a starting set. The final spectral parameters of both samples are reported in Table 1. A total of 164 and 158 experimental lines, respectively, were assigned over about 170 calculated transitions. This leaves little room for uncertainties about the "quality" of the spectral analysis. Therefore D_{HH} couplings and chemical shifts have been kept constant in the analysis of satellite spectra, where the assigned/total transition ratio is much lower. Trial D_{HC} couplings, calculated from the D_{HH} set using a crude conformational model (but including vibrational corrections) have then been used as the starting values for the analysis of the satellite spectra. To speed up and facilitate the procedure, ARCANA has been ad hoc modified to display calculated spectra including transitions from all the isotopomer spin systems, with properly scaled intensities. The program allows the use of color-coded marks on satellite lines to facilitate the assignment/deletion procedure. Once some confidence is reached about the quality of the D_{HC} couplings, such an extended data set is used to refine the conformational model. With the new set of calculated D_{HC}, spectral analysis is restarted and the process repeated until all the satellite spectra are clearly recognized (i.e., a great number of lines for each spectrum are recognized and assigned). Finally the standard spectral analysis procedure is followed paying great care that at the end (a) all experimentally observed transitions are assigned and (b) no calculated transition with intensity greater than a given threshold

TABLE 1: Spectral Parameters from the Analysis of 2,2′-Bithiophene Dissolved in ZLI1132 and I52

		D_{ij}/Hz			
ij	J_{ij}/Hz[a]	I52		ZLI1132	
$H_{11}-H_{12}$	3.8	−2261.91	± 0.02	−2742.66	± 0.03
$H_{11}-H_{13}$	1.3	−117.85	± 0.06	−194.74	± 0.09
$H_{11}-H_{14}$	0.0	−774.29	± 0.05	−876.63	± 0.06
$H_{11}-H_{15}$	0.0	−201.26	± 0.02	−219.12	± 0.03
$H_{11}-H_{16}$	0.0	−236.01	± 0.02	−267.12	± 0.04
$H_{12}-H_{13}$	5.0	766.04	± 0.04	786.22	± 0.07
$H_{12}-H_{15}$	0.0	−89.77	± 0.05	−99.97	± 0.08
$H_{12}-H_{16}$	0.0	−89.96	± 0.02	−104.39	± 0.04
$H_{13}-H_{16}$	0.0	−75.04	± 0.02	−91.24	± 0.03
$\nu_{11}-\nu_{12}$/Hz		−211.46	± 0.04	−218.51	± 0.10
$\nu_{11}-\nu_{13}$/Hz		159.25	± 0.04	247.91	± 0.10
RMS/Hz			0.15		0.22
C_2-H_{11}	5.1	262.7	± 0.2	321.1	± 0.3
C_2-H_{12}	11.8	−243.7	± 0.3	−267.9	± 0.4
C_2-H_{13}	3.0	−216.9	± 0.1	−267.4	± 0.2
C_2-H_{14}	5.4	−160.9	± 0.3	−152.1	± 0.3
C_2-H_{15}	1.4	−101.5	± 0.3	−113.3	± 0.4
C_2-H_{16}	0.4	−88.3	± 0.1	−107.8	± 0.1
RMS/Hz			0.93		0.97
C_3-H_{11}	169.0	1709.5	± 0.2	1311.3	± 0.2
C_3-H_{12}	5.6	−1043.0	± 0.2	−1183.4	± 0.2
C_3-H_{13}	9.2	−111.1	± 0.2	−158.2	± 0.2
C_3-H_{14}	0.0	−144.5	± 0.2	−157.0	± 0.3
C_3-H_{15}	0.0	−56.3	± 0.3	−60.2	± 0.3
C_3-H_{16}	0.0	−58.4	± 0.2	−68.0	± 0.1
RMS/Hz			0.89		0.95
C_4-H_{11}	5.1	−470.7	± 0.2	−648.2	± 0.2
C_4-H_{12}	169.0	−4054.4	± 0.1	−4154.8	± 0.2
C_4-H_{13}	5.1	11.2	± 0.1	−88.1	± 0.2
C_4-H_{14}	0.0	−80.1	± 0.3	−88.1	± 0.3
C_4-H_{15}	0.0	−33.4	± 0.3	−36.8	± 0.3
C_4-H_{16}	0.0	−31.8	± 0.2	−37.9	± 0.2
RMS/Hz			0.94		0.98
C_5-H_{11}	10.6	−25.4	± 0.3	−60.9	± 0.3
C_5-H_{12}	6.8	199.2	± 0.2	259.1	± 0.3
C_5-H_{13}	187.0	−5367.8	± 0.1	−7039.2	± 0.2
C_5-H_{14}	0.0	−89.2	± 0.3	−98.7	± 0.3
C_5-H_{15}	0.0	−33.4	± 0.3	−41.7	± 0.3
C_5-H_{16}	0.0	−28.9	± 0.1	−33.9	± 0.1
RMS/Hz			0.92		0.90

[a] Kept fixed in the analysis of the anisotropic spectra.

depending on S/N ratio, is unaccounted for (assigned, hidden under ^{1}H lines or summed up with transitions from other ^{13}C satellites). Both conditions are easily verified thanks to the graphic features implemented in ARCANA.

The final spectral parameters and the relative RMS values are reported in Table 1. Out of about 300 calculated transitions for each satellite, a total of 207 and 183 lines were assigned for the C_5 satellite, 202 and 194 for C_4, 169 and 178 for C_3, and 129 and 190 for C_2 for the I52 and ZLI1132 solutions, respectively. The J_{ij}'s have been kept fixed at their isotropic values.

2.2. Quantum Chemical Calculations. As discussed in section 3.1, the vibrational correction procedure relies on the availability of good force fields, either experimental or theoretical. For 2,2′-bithiophene, calculations produced a variety of $U_{\text{int}}(\{\phi\})$ with minima falling in the $31° \le \phi_{\text{min}}^{\text{syn}} \le 46°$ and $17° \le \phi_{\text{min}}^{\text{anti}} \le 42°$ range, as reported in refs 9 and 40. The DFT approach tends to predict more planar geometries, whereas MP2 calculations more distorted ones. The basis sets too play a relevant role (about 5−6° on the minima positions).

Therefore, we chose to rely for theoretical geometry optimizations and subsequent vibrational analysis on four different combinations of electron correlation method and basis set:

TABLE 2: Theoretical Internal Coordinates between the Two Thiophene Rings[a]

	B^s	B^e	MP^s	MP^e
$r_{C_1C_2}$/Å	1.453	1.453	1.452	1.455
$(\angle_{C_1C_2C_3})_{syn}$/deg	127.7	127.7	127.2	127.1
$(\angle_{C_1C_2C_3})_{trans}$/deg	129.1	129.1	128.5	128.3
ϕ_{min}^{syn}/deg	29.5	33.0	41.6	44.8
ϕ_{min}^{anti}/deg	21.6	26.3	36.8	40.6

[a] B^s, B3LYP/6-31G*; B^e, B3LYP/6-311++G**; MP^e, MP2/6-31G*; MP^e, MP2/6-311++G**.

- B^s: B3LYP method and 6-31G* basis
- B^e: B3LYP method and 6-311++G** basis
- MP^s: MP2 method and 6-31G* basis
- MP^e: MP2 method and 6-311++G** basis

Their selection was based on a compromise between accuracy and computational feasibility. The MP2 method is probably more accurate than B3LYP for the torsion potential but requires a larger and more flexible basis set to achieve properly converged results.[9,40,41] A recent survey of the MP2 and B3LYP methods in the determination of molecular equilibrium geometries[42] has revealed root-mean-square deviations of 0.008 and 0.004 Å for C−C bonds lengths, using the 6-311++G** basis set. These methods are also remarkably accurate for the calculation of molecular vibrations. Recommended scaling factors for the vibrational frequencies are 0.9496 for MP2/6-311++G**[43] and 0.9679 for B3LYP/6-311++G**.[44] Note that the relatively cheap and widely applied 6-31G* basis set is known to be unreliable for the torsion potential itself.[9] However, it is interesting to assess whether its description of equilibrium geometries (bond lengths and angles) and vibrations is good enough for the analysis of our experimental data.

We used both the Gaussian[45] and Gamess-US[46] program packages. The parallel capabilities of Gamess-US were especially important for the MP2/6-31++G** calculations. Also, we followed two different strategies for the treatment of symmetry and interfacing of the quantum chemical results with a homemade program for conformational analysis (see section 2.3). In one case, the C_2 point group symmetry was maintained, locating the origin of the system at the middle of the $\overline{C_1C_2}$ bond. The bond itself is directed along the *a* axis and the C_2 symmetry element is fixed along the *c* axis (see Figure 1). In the other case, no symmetry constraints were imposed in the optimization process, and the final coordinates and normal mode Cartesian displacements, $w_{i\xi}^{\nu}$ (section 3.1), were properly translated and rotated back to the starting reference system. In all of our test calculations, no significant differences were observed between the two programs or strategies.

The internal geometrical parameters of the thiophene rings are reported in Tables 4 and 5 for the anti-gauche conformer. The values for the syn-gauche conformer are very similar. The inter-ring geometrical parameters $r_{C_1C_2}$, $\angle_{C_1C_2C_3}$, and ϕ_{min} are reported in Table 2. Note the significant spreading of ϕ_{min} with the method and basis dimensions, as previously remembered.

2.3. Conformational Analysis. Conformational analysis was performed by AnCon, a user-friendly graphical program developed in our laboratory, which uses the gradients algorithm to minimize the error function $\text{RMS} = \sqrt{\sum(D^{\text{calc}}-D^{\text{obs}})^2/N(N-1)}$, where N is the number of independent D_{ij}'s. To perform vibrational corrections, AnCon has been interfaced with the Gaussian[45] and Gamess-US[46] suites to read Cartesian force fields (and the relative calculated vibrational frequencies, ω_ν) so as to produce the covariance-matrix elements, $C_{\alpha\beta}^{ij}$ (see below). AnCon has also been interfaced with MOLDEN[47] for interactive

TABLE 3: Experimental and Theoretical Vibrational Frequencies (cm^{-1}) of 2,2′-Bithiophene[a]

	B3LYP/6311++G** [c]		MP2/6311++G** [c]	
expt[b]	syn-gauche	anti-gauche	syn-gauche	anti-gauche
3107	3246	3246	3274	3274
3104	3245	3246	3274	3274
3080	3212	3210	3250	3247
3076	3211	3210	3248	3247
3074	3198	3197	3235	3232
3064	3197	3197	3233	3232
1557	1581	1591	1575	1582
1498	1547	1543	1514	1511
1446	1480	1481	1470	1472
1413	1453	1460	1450	1455
1383[d]	1379	1394	1396	1405
1325	1377	1353	1379	1355
1250	1270	1274	1281	1283
1227	1255	1226	1254	1254
1205	1178	1225	1204	1225
1083	1107	1107	1102	1102
1078	1101	1102	1101	1100
1056	1066	1071	1079	1084
1047	1057	1067	1064	1075
894	919	912	939	923
894	912	910	887	888
893[d]	912	901	880	875
863	859	858	868	863
843[d]	841	838	863	859
826	839	827	802	795
815	826	826	793	791
752[d]	745	741	770	769
740	741	737	764	766
703	699	698	681	694
691[d]	696	694	675	679
675	637	681	659	674
608[d]	632	612	639	623
587[d]	588	591	548	559
567[d]	575	574	547	521
523[d]	519	524	492	475
458	475	468	473	472
359[d]	334	374	327	363
284[d]	624	288	326	292
280[d]	282	279	278	273
118[d]	113	123	102	102
108[d]	109	111	98	101
37[d,e]	43	36	45	51

[a] Experimental values are for the anti-gauche conformer [b] Experimental values from ref 48. [c] This work. [d] Calculated at the RHF level of theory[67] and corrected according to ref 68. [e] Torsion.

preparation of the geometry input files (in common with the quantum chemical packages) and visualization of the outputs.

3. Results and Discussion

3.1. Vibrational Problem. For "rigid" molecules, vibrational corrections must to be considered if the correct equilibrium structure (r_e) is to be determined. As discussed in ref 35, under the assumption that vibromers share the same set of Saupe order parameters, **S**, the generic dipolar coupling can be written as

$$D = -K\sum_{r}\sum_{\zeta\xi} S_{\zeta\xi}\Phi^{r}_{\zeta\xi} \tag{1}$$

with $r = e, h$, and a corresponding to the equilibrium structure, the harmonic and the anharmonic corrections. The latter is usually neglected. $\Phi^{e}_{\zeta\xi}$ is given by

$$\Phi^{e}_{\zeta\xi} = D^{e}_{ij,\zeta\xi} = -K\frac{x_\zeta x_\xi}{r_{ij}^{5}} \tag{2}$$

with r_{ij} the internuclear distance, x_ζ its ζth component in the molecular frame, and K being related to the product of nuclear magnetogyric ratios γ_i. $\Phi^{h}_{\zeta\xi}$ depends on θ_ζ, the cosine directors between the internuclear axis and the molecular fixed frame ζ, as well as on the covariance matrix elements $C_{\zeta\xi}$ according to

$$\Phi^{h}_{\zeta\xi} = \frac{\left[C_{\zeta\xi} - 5\sum_{\gamma}\theta_\zeta(C_{\zeta\gamma}\theta_\xi + C_{\xi\gamma}\theta_\zeta) + \frac{5}{2}\theta_\zeta\theta_\xi\sum_{\gamma\eta}C_{\gamma\eta}(7\theta_\gamma\theta_\eta - \delta_{\gamma\eta})\right]}{r_{ij}^{5}} \tag{3}$$

The covariance matrix elements are in turn calculated from the vibrational frequencies, ω_ν, and the relative normal mode Cartesian displacements, $w^{\nu}_{i\zeta}$, as follows:

$$C^{ij}_{\zeta\xi} = \sum_{\nu=1}^{3N-6}(w^{\nu}_{i\zeta} - w^{\nu}_{j\zeta})(w^{\nu}_{i\xi} - w^{\nu}_{j\xi})\frac{A}{\omega_\nu}\coth\left(\frac{B\omega_\nu}{T}\right) \tag{4}$$

T being the temperature, $A = h/8\pi^2c$, and $B = ch/2k_B$, where c is the velocity of light and k_B is the Boltzmann constant.

TABLE 4: Internal Coordinates of the Thiophene Ring Subnit, Iterating on the Whole Set of Internal Coordinates (Fixing $r_{C_3H_{11}}$) and Three Order Parameters[a]

	B^s	I52	ZLI1132	B^e	I52	ZLI1132
$r_{C_2C_3}$/Å	1.378	1.401(3)	1.381(2)	1.375	1.397(3)	1.377(2)
$r_{C_3C_4}$/Å	1.424	1.446(4)	1.438(3)	1.423	1.442(4)	1.434(3)
$r_{C_4C_5}$/Å	1.368	1.391(2)	1.380(1)	1.363	1.387(2)	1.383(1)
$r_{C_5H_{13}}$/Å	1.082	1.093(3)	1.081(1)	1.079	1.090(3)	1.078(1)
$r_{C_4H_{12}}$/Å	1.085	1.087(2)	1.082(1)	1.082	1.084(2)	1.078(1)
$r_{C_3H_{11}}$/Å	1.0849	1.0849[b]	1.0849[b]	1.0822	1.0822[b]	1.0822[b]
$\angle_{C_2C_3C_4}$/deg	113.5	112.2(1)	113.0(1)	113.5	112.2(1)	113.1(1)
$\angle_{C_3C_4C_5}$/deg	112.9	112.6(2)	112.5(1)	112.9	112.6(2)	112.4(1)
$\angle_{C_4C_5H_{13}}$/deg	128.5	127.6(3)	128.0(1)	128.6	127.6(3)	127.9(2)
$\angle_{C_3C_4H_{12}}$/deg	123.7	123.2(1)	123.7(1)	123.8	123.2(1)	123.7(1)
$\angle_{C_2C_3H_{11}}$/deg	122.5	123.0(1)	122.6(1)	122.5	123.0(1)	122.6(1)
$S_{a'a'}$		−0.2881	−0.3436		−0.2891	−0.3450
$S_{b'b'} - S_{c'c'}$		0.5257	0.5950		0.5202	0.5861
$S_{a'b'}$		0.0133	−0.0132		0.0133	−0.0131
RMS		0.54	0.31		0.54	0.33

[a] Theoretical values for the *anti*-gauche conformer at B3LYP/6-31G* (B^s) and B3LYP/6-311++G** (B^e) level. [b] Kept fixed at the respective theoretical values.

TABLE 5: Internal Coordinates of the Thiophene Ring Subunit, Iterating on the Whole Set of Internal Coordinates (Fixing $r_{C_3H_{11}}$) and Three Order Parameters[a]

	MP^s	I52	ZLI1132	MP^e	I52	ZLI1132
$r_{C_2C_3}$/Å	1.385	1.404(3)	1.384(2)	1.390	1.403(3)	1.384(2)
$r_{C_3C_4}$/Å	1.415	1.449(5)	1.442(2)	1.417	1.449(5)	1.442(2)
$r_{C_4C_5}$/Å	1.378	1.393(2)	1.383(1)	1.384	1.393(2)	1.383(1)
$r_{C_5H_{13}}$/Å	1.083	1.094(3)	1.082(1)	1.082	1.094(3)	1.083(1)
$r_{C_4H_{12}}$/Å	1.085	1.090(2)	1.085(1)	1.084	1.089(2)	1.084(1)
$r_{C_3H_{11}}$/Å	1.0861	1.0861[b]	1.0861[b]	1.0853	1.0853[b]	1.0853[b]
$\angle_{C_2C_3C_4}$/deg	113.5	112.1(1)	112.9(1)	112.8	112.1(1)	112.9(1)
$\angle_{C_3C_4C_5}$/deg	112.6	112.7(1)	112.6(1)	112.4	112.7(2)	112.6(1)
$\angle_{C_4C_5H_{13}}$/deg	128.2	127.8(1)	128.1(1)	128.2	127.8(3)	128.1(1)
$\angle_{C_3C_4H_{12}}$/deg	124.3	123.2(1)	123.7(1)	124.5	123.2(1)	123.7(1)
$\angle_{C_2C_3H_{11}}$/deg	122.2	123.0(1)	122.6(1)	122.2	123.0(1)	122.7(1)
$S_{a'a'}$		−0.3035	−0.3636		−0.3085	−0.3702
$S_{b'b'} - S_{c'c'}$		0.5269	0.5812		0.5109	0.5735
$S_{a'b'}$		0.0137	−0.0140		0.0137	−0.0143
RMS		0.57	0.25		0.58	0.25

[a] Theoretical values for the anti-gauche conformer at MP2/6-31G* (MP^s) and MP2/6-311++G**(MP^e) level. [b] Kept fixed at the respective theoretical values.

A subset of the vibrational frequencies of 2,2′-bithiophene are available from IR and Raman spectroscopy,[48] for the anti-gauche conformation. These are reported in Table 3. A slightly different set of experimental data is given is ref 49, which includes solid state phonon frequencies measured by neutron scattering. Again, however, these are limited to the anti-gauche conformer. Besides, the normal modes $w_{i\xi}^{\nu}$ are not experimentally accessible (even though they are indirectly related to quantities such as Raman and IR intensities). For this reason vibrational frequencies and normal modes of both conformers must be calculated by some quantum chemical method, as eigenvalues and eigenvectors of the force field (FF) matrix. The availability of good force fields has been in the past a limiting factor, but it has been shown (see refs 43, 44, 50, and 51 and references therein) that density functional methods or similar high-level approaches can successfully predict vibrational spectra of fairly large systems.

The mixed approach[52,53] (calculated normal modes and experimental frequencies) was eventually adopted in calculating the covariance matrix elements, $C_{\xi\xi}^{ij}$, of eq 4. Taking into account that (a) only the experimental vibrational frequencies of the anti-gauche conformer are available and (b) differences between experimental and calculated values for the anti-gauche conformer are greater than the calculated values for the two conformers, at least at the levels of approximation used, we decided to use the same experimental set for both conformers.

3.2. Geometry of the Thiophene Subunit. As a preliminary step, the geometry of the thiophene ring fragment has been investigated. Locating a Cartesian system on the fragment with the origin on the C_2 nucleus, the a' axis along the $\overline{C_2C_3}$ bond and the b' axis lying on the ring plane (see Figure 1), three independent S elements and 10 geometrical parameters are to be determined against 15 D_{ij}'s. Note that one bond length ($r_{C_3H_{11}}$ in this case) must be kept fixed at a theoretical value so as to avoid the "scaling effect" with the order parameter. Now eq 1 holds and so the standard procedure for vibrational corrections can be followed, the AnCon interface with MOLDEN keeping track of the spatial relationship between the fragment and the molecule-fixed Cartesian system to apply correctly the normal mode displacements. Calculations were performed using the anti-gauche conformer FF to calculate the covariance matrix not including the internal rotation frequency $\omega_v = 37$ cm^{-1}. Distances and bond angles calculated by iterating on the full set of 13 variables are reported in Tables 4 and 5. Calculations were repeated by iterating cyclically on subsets of parameters, but the calculated ratios differ on the third decimal digit with respect to the reported values. In Table 6 harmonic corrections, absolute ($\Delta = D^{calc} - D^{obs}$) and relative ($\Delta/D^{e}$) errors on direct couplings are reported for the MP^e case in ZLI1132. Very similar results are obtained also for the I52 data and the other theoretical approaches. Both kinds of errors are well spread, the worst absolute error a conspicuous 1.84 Hz for $D_{3,13}$ in I52 and B^e; the small $D_{5,11}$ coupling is affected by the largest relative error in all cases. Note also the high vibrational correction calculated for $^2D_{3,12}$ and $^3D_{11,12}$, the latter a D_{HH} coupling. Harmonic corrections ranging from 405.25 Hz (MP^s) up to 414.74 Hz (MP^e) in ZLI1132 (386.03 and 394.73 Hz, respectively, in I52) for $^1D_{4,12}$ or from 792.91 Hz (MP^e) to 807.48 Hz (B^e) in ZLI1132 (594.09 and 604.21 Hz, respectively, in I52) for $^1D_{5,13}$ were calculated.

The analysis of distance ratios with respect to $r_{C_2C_3}$ or $r_{C_3H_{11}}$ (upper and lower half of Table 7) reveals that the largest differences are observed between the two phases, rather than from the use of different FF. ZLI1132 produces values slightly closer to the calculated ones, but the differences are very near or within the standard deviations. In all cases, LXNMR gives a $r_{C_3C_4}$ distance much longer than the calculated one.

TABLE 6: D^h, Absolute and Relative Error on $D_{calc} = D^e + D^h$ from the Optimization of the Thiophenic Ring Fragment

	ZLI1132			
ij	D_{calc}/Hz	D^h/Hz	Δ^a/Hz	(Δ/D^e)/%
2, 11	320.92	−2.57	−0.18	−0.05
2, 12	−268.27	7.06	−0.37	0.13
2, 13	−267.46	7.17	−0.06	0.03
3, 11	1311.32	−52.02	0.02	0.00
3, 12	−1183.53	45.32	−0.13	0.01
3, 13	−158.61	3.71	−0.41	0.25
4, 11	−648.42	25.05	−0.22	0.03
4, 12	−4154.78	414.74	0.02	−0.00
4, 13	−87.98	0.01	0.12	−0.13
5, 11	−60.29	1.68	0.760	−0.97
5, 12	259.24	−6.97	0.14	0.05
5, 13	−7039.20	792.91	0.00	−0.00
11, 12	−2742.53	75.20	0.13	−0.00
11, 13	−195.09	4.51	−0.28	0.14
12, 13	786.15	−3.46	−0.07	−0.01

[a] $\Delta = D_{calc} - D_{obs}$.

Note that an "averaged" structure is calculated; even if theoretical calculations predict a very small dependence of the ring subunit geometries on ϕ, the combined effect of different orientation and geometries can produce significative "apparent" distortions of the rigid subunit. Also the effect of neglecting the contribution of the syn-gauche FF should be considered in this case because now the contribution of this conformer is expected to be significant. Calculations repeated using theoretical rather than experimental frequencies gave very similar results with slightly higher RMS values.

3.3. Conformational Analysis: The AP Approach. In a molecule undergoing large amplitude motions, the dipolar couplings are averaged according to

$$D_{ij}^{e} = D_{ijZZ} = \int P_{LC}^{\{\phi\}} \sum_{\zeta\xi} S_{\zeta\xi}(\{\phi\}) D_{ij,\zeta\xi}^{e}(\{\phi\})\, d\{\phi\} \quad (5)$$

where $P_{LC}^{\{\phi\}}$ is the conformer distribution function in the anisotropic medium, $D_{ij,\zeta\xi}^{e}$ is defined in eq 2, and $\{\phi\}$ describes the internal coordinates subset defining the relative motions of the rigid subunits the molecule is made up. For 2,2′-bithiophene $\{\phi\}$ reduces to the dihedral angle ϕ of Figure 1.

To investigate the conformational equilibrium, three points have to be taken into account: (a) a way to describe the dependence of the order parameters **S** on $\{\phi\}$, (b) a way to parametrize $P_{LC}^{\{\phi\}}$ (or better $p^{\{\phi\}}$, the isotropic conformer distribution function), and (c) a procedure to deal with vibrational corrections in the presence of large amplitude, torsional motions.

Dependence of S on $\{\phi\}$. The order parameters are given by

$$S_{\xi\zeta}(\{\phi\}) = \frac{1}{Z(\{\phi\})} \int \left(\frac{3\cos\theta_\xi \cos\theta_\zeta - \delta_{\xi\zeta}}{2} \right) \exp\{-U_{ext}(\beta,\varphi,\{\phi\})/kT\} \sin\beta\, d\beta\, d\varphi \quad (6)$$

with

$$Z(\{\phi\}) = \int \exp\{-U_{ext}(\beta,\varphi,\{\phi\})/kT\} \sin\beta\, d\beta\, d\varphi \quad (7)$$

θ_ξ is the angle between molecular ξ and the Z laboratory axes, β and φ are the polar and azimutal angles defining the direction of the mesophase director d with respect to the molecular system. $U_{Tot}(\beta,\varphi,\{\phi\})$, the singlet total orientational energy, can

TABLE 7: Distance Ratios with Respect to $r_{C_2C_3}$ (Upper) and $r_{C_3H_{11}}$ (Lower) from the Optimization of the Thiophene Ring Fragment[a]

	calc				I52				ZLI1132				
	B^s	B^e	MP^s	MP^e	B^s	B^e	MP^s	MP^e	B^s	B^e	MP^s	MP^e	$\times 10^{-3}$ [b]
$r_{C_2C_3}$	1.000	1.000	1.000	1.000	1.017	1.016	1.014	1.009	1.002	1.001	0.999	0.996	± 3
$r_{C_3C_4}$	1.033	1.035	1.022	1.019	1.049	1.049	1.046	1.042	1.043	1.043	1.041	1.037	±5
$r_{C_4C_5}$	0.993	0.993	0.995	0.996	1.009	1.009	1.006	1.002	1.001	1.001	0.998	0.995	±2
$r_{C_5H_{13}}$	0.785	0.785	0.781	0.778	0.793	0.793	0.790	0.787	0.784	0.784	0.781	0.779	±3
$r_{C_4H_{12}}$	0.787	0.787	0.783	0.780	0.789	0.788	0.787	0.783	0.785	0.784	0.783	0.780	±2
$r_{C_3H_{11}}$	0.787	0.787	0.784	0.781	0.787	0.787	0.784	0.781	0.787	0.787	0.784	0.781	
$r_{C_2C_3}$	1.271	1.271	1.275	1.281	1.291	1.291	1.293	1.293	1.273	1.273	1.274	1.275	±3
$r_{C_3C_4}$	1.314	1.315	1.303	1.306	1.333	1.333	1.334	1.335	1.325	1.325	1.328	1.329	±5
$r_{C_4C_5}$	1.262	1.262	1.269	1.276	1.282	1.282	1.283	1.284	1.278	1.273	1.273	1.275	±2
$r_{C_5H_{13}}$	0.998	0.997	0.997	0.997	1.007	1.007	1.007	1.008	0.996	0.996	0.996	0.998	±3
$r_{C_4H_{12}}$	1.001	1.000	0.999	0.999	1.002	1.002	1.004	1.004	0.997	0.996	0.999	0.999	±2
$r_{C_3H_{11}}$	1.000	1.000	1.000	1.000	1.000	1.000	1.000	1.000	1.000	1.000	1.000	1.000	

[a] B^s, B3LYP/6-31G*; B^e, B3LYP/6-311++G**; MP^s, MP2/6-31G*; MP^e, MP2/6-311++G**. [b] The largest standard deviation for each parameter.

be written as

$$U_{Tot}(\beta,\varphi,\{\phi\}) = U_{ext}(\beta,\varphi,\{\phi\}) + U_{int}(\{\phi\}) \quad (8)$$

with $U_{ext}(\beta,\varphi,\{\phi\})$ the anisotropic, intermolecular, potential and $U_{int}(\{\phi\})$ the internal rotational potential. $U_{ext}(\beta,\varphi,\{\phi\})$ is approximated[54] to

$$U_{ext}(\beta,\varphi,\{\phi\}) = -\epsilon_{2,0}(\{\phi\})D^2_{0,0}(\theta,\varphi) - 2\epsilon_{2,2}(\{\phi\})\mathrm{Re}\{D^2_{0,2}(\theta,\varphi)\} \quad (9)$$

where the $\epsilon_{2,m}(\{\phi\})$, elements of the molecule solute−solvent interaction tensor expressed with respect to the principal axes for each conformation $\{\phi\}$, according to the additive potential (AP) model,[36] are in turn given by

$$\epsilon_{2,m}(\{\phi\}) = \sum_p \sum_j \epsilon^j_{2,p}\, D^2_{p,m}(\{\Omega^j_\phi\}) \quad (10)$$

and the Wigner rotation matrix $D^2_{p,m}(\{\Omega^j_\phi\})$ relates the principal axes of ϵ^j to the molecular reference frame. In this way it is possible to give a continuous dependence of the order parameters over the set of internal coordinates, with $\epsilon^j_{2,p}$, elements of the conformationally independent interaction tensor of the jth fragment, as adjustable parameters.

As a way to get rid of the complications associated with the vibrational correction procedure, preliminary calculations were carried out by including in the experimental set only those D_{ij} couplings whose D^h contributions are expected to be small. Because usually the D_{HH} couplings are assumed to be little affected by vibrational corrections, the smallest of such set should be obviously composed of the 9 D_{HH} couplings (but note the 3% contribution to $D_{11,12}$). With (i) the AP approximation to describe the coupling between orientational and internal motions and (ii) the previously found geometry for the thiophene rings, five parameters ($r_{C_1C_2}$ and the $\angle_{C_1C_2C_3}$ angle plus three ϵ values: $\epsilon^{C_2C_3}_{2,0}$, $\epsilon^{C_3C_4}_{2,0}$, $\epsilon^{CH}_{2,0}$) are needed if one of the theoretical $U_{int}(\{\phi\})$ reported in Raos et. al.[9] could reproduce the 2,2′-bithiophene conformational equilibrium in a condensed fluid phase. Unfortunately, notwithstanding the very small overdeterminacy, the RMS error never gets lower than 4 Hz with also unacceptably short $r_{C_1C_2}$ distances (1.38 Å). Higher RMS values are obtained when all the *inter*-ring D_{ij} couplings and the *intra-ring* couplings with vibrational corrections less than 1% were used.

Parametrization of $p^{\{\phi\}}$. To proceed further in the conformational analysis, a suitable way to parametrize $P^{\{\phi\}}_{LC}$ of eq 5 has to be found. Here a novel approach giving the conformer probability distribution function as a sum of a minimal set of weighted Gaussian functions will be followed.[37] In this way, a more accurate description of the relevant parts of the potential function can be achieved with a lower number of adjustable parameters with respect to the expansion of the internal rotation function in a truncated Fourier series. Accordingly, the 2,2′-bithiophene probability distribution function p^ϕ can be described by a linear combination of two Gaussians for a total of five parameters (the ϕ^{syn} and ϕ^{anti} angles, the h^{syn} and h^{anti} widths plus the p^{anti} population):

$$p^\phi = \frac{p^{anti}}{\pi^{1/2}h^{anti}} \exp\left\{-\left(\frac{\phi+\phi^{anti}-\pi}{h^{anti}}\right)^2\right\} + \frac{1-p^{anti}}{\pi^{1/2}h^{syn}} \exp\left\{-\left(\frac{\phi-\phi^{syn}}{h^{syn}}\right)^2\right\} \quad (11)$$

Vibrational Corrections for Flexible Molecule. Equation 1 can be easily generalized to flexible molecules becoming

$$D \simeq -K\int p^\phi \sum_r \sum_{\zeta\xi} S^\phi_{\zeta\xi}(\Phi^r_{\zeta\xi})^\phi\, d\phi \quad (12)$$

which reduces to

$$D \simeq -K \sum_n^{N.Conf} p^n \sum_r \sum_{\zeta\xi} S^n_{\zeta\xi}(\Phi^r_{\zeta\xi})^n \quad (13)$$

in the RIS approximation. Note the dependence of the Saupe matrix and $\Phi^h_{\zeta\xi}$ on the internal coordinate set $\{\phi\}$ and note that to apply eq 12, the continuous dependence of FF on $\Phi^r_{\zeta\xi}$ is required. On the contrary, if eq 13 holds, only the FF of conformers corresponding to minima of $U_{int}(\{\phi\})$ are needed. It is impractical, if not impossible, to obtain a continuous dependence of the FF on $\{\phi\}$ for a molecule as complex as 2,2′-bithiophene. Thus, if we want to use a continuous description of the potential barrier, some approximations have to be introduced in eq 12.

As implicitly done by Diehl et al.[55] for benzaldehyde, $\Phi^r_{\zeta\xi}$ can be evaluated at each $\{\phi\} \neq \{\phi_n\}$ from covariance matrices $\mathbf{C}^n_{\zeta\xi}$ calculated for the conformers corresponding to $\{\phi_n\}$, the minima of $U_{int}(\{\phi\})$. The increasing error on the vibrational corrections will be quickly annihilated by the Boltzmann factor $p^{\{\phi\}}$ when $\{\phi\}$ is moving away from $\{\phi_n\}$. In this way only FF of conformers corresponding to the minima of $U_{int}(\{\phi\})$ are needed. We will refer to this scheme as Approximation I. There

TABLE 8: Internal Coordinates and Potential and Orientational Parameters from the Optimization of the Full Molecule

	I52				ZLI1132			
	B^s	B^e	MP^s	MP^e	B^s	B^e	MP^s	MP^e
$r_{C_2C_3}$/Å	1.400(3)	1.395(2)	1.401(2)	1.400(3)	1.381(5)	1.377(5)	1.381(5)	1.380(5)
$r_{C_3C_4}$/Å	1.444(4)	1.439(1)	1.445(4)	1.444(4)	1.437(7)	1.432(7)	1.437(7)	1.436(7
$r_{C_4C_5}$/Å	1.390(1)	1.386(1)	1.391(1)	1.390(1)	1.382(3)	1.378(3)	1.382(3)	1.381(3)
$r_{C_5H_{13}}$/Å	1.092(2)	1.089(2)	1.092(2)	1.092(2)	1.082(2)	1.079(3)	1.082(4)	1.082(4)
$r_{C_4H_{12}}$/Å	1.088(2)	1.084(2)	1.090(2)	1.089(2)	1.079(2)	1.076(3)	1.081(3)	1.080(4)
$r_{C_3H_{11}}$[a]/Å	1.0849	1.0822	1.0861	1.0853	1.0849	1.0822	1.0861	1.0853
$\angle_{C_2C_3C_4}$/deg	112.2(1)	112.2(1)	112.2(1)	112.2(1)	112.9(2)	113.0(2)	112.9(2)	112.9(2)
$\angle_{C_3C_4C_5}$/deg	112.7(1)	112.6(1)	112.7(1)	112.7(1)	112.3(2)	112.3(2)	112.4(2)	112.4(2)
$\angle_{C_4C_5H_{13}}$/deg	127.8(2)	127.7(2)	127.9(2)	127.9(2)	127.7(4)	127.8(4)	127.8(4)	127.8(4)
$\angle_{C_3C_4H_{12}}$/deg	123.3(1)	123.3(1)	123.3(1)	123.2(1)	123.8(2)	123.8(2)	123.8(2)	123.8(2)
$\angle_{C_2C_3H_{11}}$/deg	123.1(1)	123.1(1)	123.1(1)	123.1(1)	122.8(1)	122.8(1)	122.8(1)	122.8(1)
$r_{C_1C_2}$/Å	1.471(2)	1.467(2)	1.470(2)	1.470(2)	1.451(4)	1.447(4)	1.452(4)	1.451(4)
$\angle_{C_1C_2C_3}$/deg	127.8(2)	127.8(2)	127.8(2)	127.8(2)	128.5(3)	128.5(3)	128.5(2)	128.5(3)
				Potential				
psyn	0.33(1)	0.33(2)	0.33(1)	0.33(1)	0.33(2)	0.33(1)	0.33(2)	0.33(1)
$h_{anti} = h_{syn}$[a]	1.7	1.7	1.7	1.7	1.7	1.7	1.7	1.7
Φ_{minsyn}/deg	22.9(5)	22.9(4)	22.8(4)	23.0(4)	22.3(7)	22.3(7)	22.4(7)	22.6(7)
$\Phi_{minanti}$/deg	23(2)	23(2)	24(2)	24(2)	24(3)	24(3)	24(3)	24(3)
				Orientational				
$\epsilon_{2,0}^{C_2C_3}$	1.07(1)	1.06(1)	1.08(1)	1.08(1)	1.13(3)	1.11(3)	1.13(3)	1.13(3)
$\epsilon_{2,0}^{C_3C_4}$	2.13(2)	2.10(1)	2.14(1)	2.13(1)	2.25(4)	2.22(4)	2.24(4)	2.25(4)
$\epsilon_{2,0}^{CH}$	−0.74(1)	−0.73(1)	−0.74(1)	−0.74(1)	−0.49(2)	−0.49(2)	−0.50(2)	−0.50(2)
RMS	0.54	0.53	0.53	0.53	0.98	0.98	0.98	0.98

[a] Kept fixed as discussed in the text.

is, however, at least one more point to be taken in account. If a general consensus were to exist on the shape of $U_{int}(\{\phi\})$, as in the case of previously recorded benzaldehyde with only a pair of planar symmetry related conformers, and Approximation I holds, then eq 12 is a simple extension of eq 1, but when the shape and/or position of the minima of the internal potential function is debated, further sources of error, whose magnitude is unclear, are introduced. In this case the possibility to produce reliable $(\Phi^h_{\xi\xi})^n$ could be questionable because (a) quantum-mechanical calculations at different level of approximation and/or basis sets produce $U_{int}(\{\phi\})$ differing in the minimum positions $\{\phi'_n\}$, (b) such values may differ in turn from $\{\phi_n\}$, the minimum positions in the nematic phase, and (c) the magnitude of the error following the substitution of $\{\phi_n\}$ for $\{\phi'_n\}$ is unknown (Approximation II). Such is the case of 2,2′-bithiophene as previously discussed.

3.4. Conformational Equilibrium of 2,2′-Bithiophene. *AP Approach*. We proceeded as follows to calculate covariance matrices: (i) Approximation I was adopted; (ii) the syn-gauche FF was used when $0° \le \phi < 90°$ and the anti-gauche FF when $90° \le \phi \le 180°$; (iii) the mixed approach was adopted; (iv) the vibrational frequency corresponding of the torsional normal mode was not included in the calculation of $C^{ij}_{\xi\xi}$ (eq 4). To test for the effects of Approximation II, a two-step procedure was adopted: calculations were first performed using the FF calculated at the theoretical $\{\phi'_n\}$ minima to obtain a set of AP's $\{\phi_n\}$; FF recalculated at the latter values were then fed back into AnCon and calculations were repeated.

In a preliminary run cycle, with the ring geometrical parameters kept fixed at the optimized geometry values of Tables 4 and 5, nine parameters (three $\epsilon^j_{2,0}$, ϕ^{syn}, ϕ^{anti}, p^{anti}, $h^{anti} = h^{syn}$, and two geometrical parameters, namely, $r_{1,2}$ and the $\angle C_1C_2C_3$ angle) are optimized against 33 D_{ij}. ϕ^{anti}, ϕ^{syn}, h^{anti}, and h^{syn} were strongly correlated; a scan in the 0.1−15.0 Hz rangeof $h^{anti} = h^{syn}$ gave low RMS errors (in the 0.5−1.4 Hz range) and small standard deviations on both ϕ^{anti} and ϕ^{syn} for $h^{anti} = h^{syn} = 1.7 \pm 1.3$ Hz. Therefore in the ensuing calculation the latter were kept fixed at 1.7 Hz. The ϕ^{syn} and ϕ^{anti} values moved significantly from the respective theoretical values only in the first of the two steps, the intermediate and final values differing within the standard deviations. In an a posteriori test, starting with the FF calculated at the AP's $\{\phi_n\}$, the same final values were calculated with a single step. We can safely conclude that vibrational corrections are quite insensitive not only to the level of theory used to calculate FF but also to the position of the $\{\phi'_n\}$ minima. For the same reasons, Approximation I too should work properly.

With these preliminary results, we performed further calculations iterating on the thiophene ring parameters too to verify the possible effects of having used only the anti-gauche FF to calculate the ring geometry. Here a cyclical iterative approach was followed to maintain a high data/parameters ratio. The results are reported in Table 8. In Table 9 D^h, Δ, and relative errors for the I52, MP^e case are reported, and the resulting conformer distribution function is plotted in Figure 3. This may be compared with the theoretical range of minimum-energy ϕ values (vertical gray bars in Figure 3) and with plots of the full gas phase torsional distribution, from the best available calculations[9] (Figure 4).

The data show clearly why none of the theoretical $U_{int}(\{\phi\})$ can fit the dipolar coupling set: note, in fact, how the value of ϕ^{syn}_{min} falls outside the theoretical range. On the contrary, ϕ^{anti}_{min} falls within the range, near the values predicted by DFT. For both conformers, a strong "flattening" effect with respect to the theoretical data for the isolated molecule is evident. No significant differences are observed between ring geometries obtained by fitting the thiophene ring as a rigid subunit (Tables 4 and 5) and the relative values of Table 8; the differences, within standard deviations, are likely due to differences in the optimization process. At least for 2,2′-bithiophene, which has a significant presence of both conformers, the data are relatively insensitive to FF with respect to this approximation too.

A more exhaustive description of the conformational equilibrium requires that the rigid rotor hypothesis be relaxed

TABLE 9: D^h, Absolute and Relative Error on $D_{calc} = D^e + D^h$ from the Optimization of 2,2′-Bithiophene by the AP Method

	I52			
ij	D_{calc}/Hz	D^h/Hz	Δ^a/Hz	(Δ/D^e)/%
2, 11	262.51	−1.42	−0.06	−0.07
2, 12	−244.04	6.09	0.19	0.14
2, 13	−217.23	6.01	−0.42	0.15
2, 14	−161.01	3.11	−0.63	−0.07
2, 15	−101.42	1.16	−0.43	−0.07
2, 16	−89.08	1.17	−1.00	0.86
3, 11	1709.44	−85.63	0.02	0.03
3, 12	−1042.66	39.31	−0.21	−0.03
3, 13	−109.27	2.73	−0.65	−1.63
3, 14	−144.96	−0.39	−0.62	0.32
3, 15	−56.41	0.22	−2.26	0.20
3, 16	−57.95	0.28	−0.09	−0.77
4, 11	−470.58	19.72	−0.28	−0.02
4, 12	−4054.41	395.70	0.02	0.00
4, 13	11.10	−1.69	−0.02	−0.76
4, 14	−79.39	−0.17	2.31	−0.89
4, 15	−33.34	0.04	−0.54	−0.17
4, 16	−31.93	0.05	0.12	0.40
5, 11	−24.93	0.99	1.24	−1.80
5, 12	199.40	−5.82	0.31	0.10
5, 13	−5367.80	601.30	0.00	0.00
5, 14	−90.53	−0.23	−1.06	1.48
5, 15	−33.14	0.02	3.62	−0.77
5, 16	−28.02	0.05	−0.26	−3.10
11, 12	−2262.07	64.12	0.19	0.01
11, 13	−118.31	3.10	0.01	0.38
11, 14	−774.26	−12.35	0.03	−0.00
11, 15	−200.97	0.04	0.47	−0.14
11, 16	−235.60	0.19	0.38	−0.17
12, 13	766.21	−4.06	−0.16	−0.02
12, 15	−89.74	0.11	0.11	−0.03
12, 16	−90.08	0.10	−0.48	0.14
13, 16	−74.99	0.17	−0.76	−0.07

[a] $\Delta = D_{calc} - D_{obs}$.

allowing for, at least, $\angle_{C_1C_2C_3}$ to assume a different value for each conformer. In fact, of all the geometrical parameters calculated at the various levels of theory, only for this angle is an appreciable difference of about 1° observed between the two conformers (Table 2). Such a difference is expected to be too small to be detected and the two angles are expected to be strongly correlated, as happens for h^{anti} and h^{syn}.

Given the very high overdeterminacy, we are quite confident to have obtained a physically sound minimum. Notwithstanding the assumptions needed to handle this complex conformational equilibrium, the value of ϕ^{syn}_{min} outside the 31−46° range reflects an effect of the solvent on the conformer structure, as observed elsewhere.[25,56,57]

RIS Approach. Even if h^{anti} and h^{syn} cannot be determined with high accuracy, the conformer distribution function is rather sharp, as shown in Figure 3; only conformers within a ±5° range about the minima contribute to D_{ij}. Therefore the approximation $U_{int}(\{\phi\}) = -\sum_n^{N.Conf} V_n \delta(\{\phi\} - \{\phi_n\})$ should hold and for 2,2′-bithiophene N.Conf = 4, i.e., two pairs of "rigid", symmetry related, conformers, each characterized by a proper $\{\phi_n\}$ and its own set of "weighted" order parameters $p^n S^n_{\zeta\xi}$. Choosing the proper molecule-fixed reference system,[27] the conformational equilibrium is determined by seven independent parameters (three $S^n_{\zeta\xi}$ for the two symmetry related syn-gauche, three for the anti-gauche conformers, and a weighting factor p^{syn}). Note that (i) there are six independent order parameters versus three independent $\epsilon^j_{2,p}$ of the AP approach and (ii) because only the products of the weight p^n times the order elements $S^n_{\zeta\xi}$ can be determined by this approach, a range of p^n giving $S^n_{\zeta\xi}$ elements within their physically allowed ranges is all that can be predicted.

No assumptions on the order parameters and/or values of ϕ_{min} as in ref 27 are needed given the very large data set available; eq 13 will hold and the vibrational correction procedure is easily applied with the covariance matrix calculated with the force field of the anti-gauche and syn-gauche conformer calculated at the respective theoretical $\{\phi'_n\}$ minima. On such a basis only, the RIS approach gives quite a large range of possible solutions in terms of $\{\phi\}$ and conformer relative weights. Then, even with such an extended data set, we could conclude that the RIS approach does not gives relevant information about the conformational equilibrium of 2,2′-bithiophene. Anyway, it is quite interesting to note that (a) the conformational hypothesis[27] with $\phi^{anti}_{min} = 0°$ can be excluded when ϕ^{syn}_{min} is outside the 15−

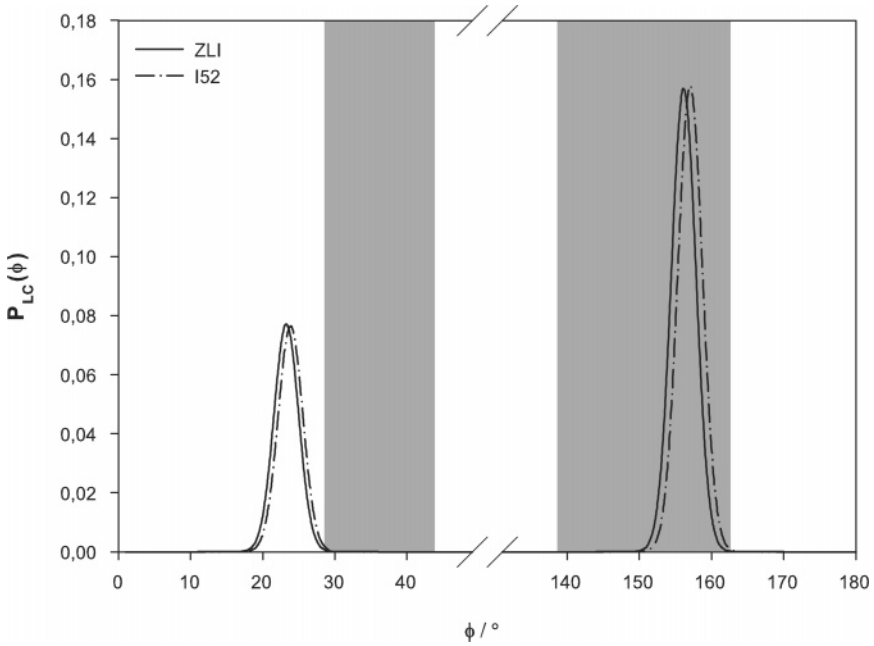

Figure 3. Conformer distribution function p^ϕ for 2,2′-bithiophene in I52 (−·−) and ZLI1132 (—). In gray is the theoretical range of ϕ (positions of energy minima) as predicted by different computational methods.[9]

TABLE 10: S_{ab} Calculated According to the RIS Model at the AP $\{\phi_{min}\}$ and Theoretical $\{\phi'_{min}\}$ Minima (AP Values at the Relative Minima Reported for Comparison)

			RIS model					
					RIS-DFT			
	AP model [a]		RIS-AP [b]		I52		ZLI1132	
order parameters	I52	ZLI1132	I52	ZLI1132	(B^s)[c]	(B^e)[d]	(B^s)[c]	(B^e)[d]
S_{aa}^{syn}	−0.1159	−0.1183	−0.1923	−0.2092	−0.4015	−0.4643	−0.4517	−0.5149
S_{ac}^{syn}	0.0025	−0−0034	0.0143	0.0150	0.1342	0.1666	0.1940	0.2363
$S_{bb}^{syn} - S_{cc}^{syn}$	0.6900	0.8028	0.7897	0.8434	0.5443	0.6315	0.3127	0.3733
S_{aa}^{anti}	−0.2858	−0.3401	−0.2886	−0.3599	−0.3531	−0.4219	−0.4033	−0.4771
S_{ac}^{anti}	0.0190	−0−0333	0.0172	−0.0347	0.0052	−0.0468	−0.0018	−0.0558
$S_{bb}^{anti} - S_{cc}^{anti}$	0.5225	0.5901	0.4730	0.5389	0.4213	0.4649	0.4223	0.4663
RMS			0.95	1.47	0.59	1.24	0.61	1.25

[a] AP model case B^e: $\{\phi_n\}$ as reported in Table 8. [b] At the same $\{\phi_n\}$ as in the AP model. [c] B^s: $\phi_{min}^{syn} = 29.5°$; $\phi_{min}^{anti} = 21.6°$ and $p^{anti} = 0.76$ as calculated at the B3LYP/6-31G* level. [d] B^e: $\phi_{min}^{syn} = 33.0°$; $\phi_{min}^{anti} = 26.3°$ and $p^{anti} = 0.75$ as calculated at the B3LYP/6-311++G** level.

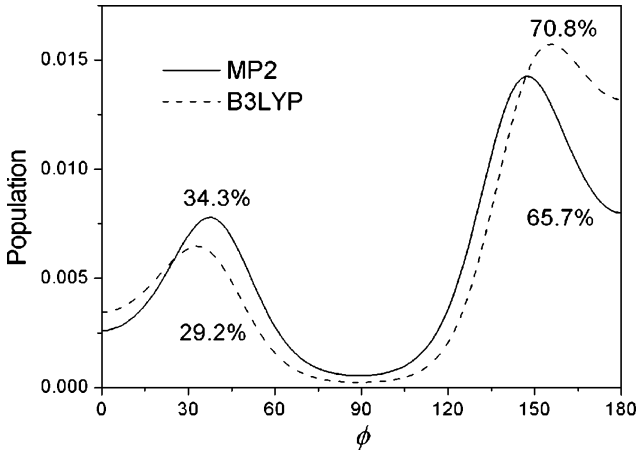

Figure 4. Theoretical conformer distribution function p^{ϕ} for 2,2′-bithiophene in the gas phase. The plots are Boltzmann populations at $T = 298$ K, calculated using MP2/aug-cc-pVTZ and B3LYP/aug-cc-pVTZ potential functions.[9] The relative weights of the syn-gauche and anti-gauche conformers, obtained by integration of the populations in the [0°, 90°] and [90°, 180°] ranges, have also been indicated.

36° range, and (b) at the MP^s and MP^e $\{\phi'_n\}$ minima, for no p^n was it possible to obtain a set of order parameters within their physically allowed range. Remembering that MP2 calculations produce $\{\phi'_n\}$ values in the upper half of the theoretical range, the latter result is clearly consistent with that found with the AP model. The same conclusions are reached for the DFT calculations too if the physical nature of the order parameters is considered. Experimental evidences have shown that shape plays a predominant role in determining the solute orientation: therefore, as correctly predicted by the AP approach, similarly large, positive S_{aa}^{syn} and S_{aa}^{anti} values (and small S_{ab}^{syn} and S_{ab}^{anti}) are expected given the prolate nature of 2,2′-bithiophene, the *a* axis of Figure 1 being nearly coincident with the long molecular axis. As shown in Table 10, this does not happen when $\{\phi'_n\}$ values from DFT quantum mechanical calculations were used. Also the $S_{bb}^{syn} - S_{cc}^{syn}$ values are quite unrealistic. On the contrary, physically meaningful $S_{\zeta\xi}^{n}$ were calculated using the $\{\phi_n\}$ from the AP, both approaches (AP and RIS) giving similar values as reported in Table 10.

4. Conclusions

A detailed and exhaustive discussion of the conformational equilibrium of 2,2′-bithiophene in a condensed, fluid phase was possible. The task has been achieved by going through the following steps:

(a) Recording and analyzing the isotropic and anisotropic spectra of 2,2′-bithiophene (section 2.1). In particular, the analysis of the ^{1}H satellite spectra due to four different ^{13}C isotopomers was possible only because very high-quality anisotropic spectra were recorded. This requisite, which applies as a general rule also for the analysis of standard ^{1}H spectra, becomes very stringent when satellites spectra are involved. This fact restricts the choice as possible solvents to a very few LCs. A graphical procedure, described in more detail elsewhere,[58] must be used to ensure the goodness of the D_{HC}.

(b) Determining the full set of vibrational frequencies, ω_ν, and the relative normal mode Cartesian displacements, $w_{i\zeta}^{\nu}$ (section 2.2). The former are usually available from literature whereas, for molecules of such complexity, $w_{i\zeta}^{\nu}$ can be obtained from the diagonalization of the force field matrices obtained by quantum mechanical calculations.[59−61] Force fields were calculated with different ab initio approaches (i.e., MP2 or B3LYP) and/or base dimensions and the differences in structure and conformational equilibrium compared with those obtained in the two solvents.

(c) Discussing a procedure to apply vibrational corrections to the flexible molecule case (section 3.3). To deal with vibrational corrections in the presence of large amplitude torsional motions, some approximations, whose magnitude and influence on the results is currently debated, have to be introduced. On the other hand, for 2,2′-bithiophene, the LXNMR minima are not fixed by symmetry and are different from those calculated theoretically, as verified using subsets of D_{ij} whose vibrational corrections are expected negligible. A "two step procedure" showed that the results are quite insensitive to the choice of the force field. It was then found that the calculated geometries depend on the different force fields and/or approximations and procedures used but the bond distance and angle values are spread within a narrow range centered on reasonable values; geometrical data can be obtained with a lower precision compared to rigid molecule cases. What is more, none of the possible choices can be safely rejected because there will always be an uncertainty about how precise a structure and conformational probability can be obtained by the LXNMR method. In this respect, the "geometry based" filter due to the presence of the D_{HC} couplings is ineffective.

(d) Discussing different conformational hypothesis. Very simple conformational equilibria can be safely rejected because they are absolutely incompatible with the D_{ij} data set; from this point of view then the presence of the D_{HC} couplings plays a fundamental role. We demonstrated also that a wide range of conformational equilibria are compatible with the RIS approach

if only the allowed mathematical range of the **S** matrix elements is used to discriminate between different equilibria. On the contrary, simple molecule-shape-based considerations on the expected values of the $S_{\alpha\beta}$ elements restricted in a significant way the range of possible conformational equilibria and, what is more, the more physically sound $S_{\alpha\beta}$ values are fully compatible with minima of $U_{int}(\{\phi\})$ outside the theoretical range.

As a first point, it is then very important to remember that a satisfactory description of the conformational equilibrium was possible only due to the presence in the experimental parameter set of the D_{HC} couplings from the analysis of the four ^{13}C satellite spectra. The shape of $U_{int}(\{\phi\})$ is qualitatively similar to the one predicted by ab initio calculations, in that an equilibrium between two pairs of symmetry-related syn-gauche and anti-gauche conformers is consistent with the experimental data. Also the population ratios are in fair agreement. On the other hand, our analysis produces a value of ϕ_{min}^{syn} outside the range of the calculated values, as illustrated in Figure 3. Also, ϕ_{min}^{anti} is significantly smaller than the MP2 predicted values. A narrowing of the torsional distribution around the potential minima is also observed in comparison with the theoretical predictions in Figure 4. Finally, whereas bond distances and angles fall in a range of values compatible with theoretical data, a significantly longer value for $r_{C_3C_4}$ is calculated (the LXNMR $r_{C_3C_4}/r_{C_2C_3}$ ratio is in the 1.037−1.049 versus the theoretical 1.019−1.035 range). From many point of view the effect seems real and clearly not a consequence of errors in spectral analysis (an eventuality difficult to be ruled out when satellite spectra are involved) because it is present in both samples.

At the moment it is unclear if the discrepancies between theory and experiment are due to the approximations in the data analysis and in the theoretical calculations or if there is a real difference due to the environment felt by the molecule (and consequently to be attributed to the chemical nature of the solvent). In a recently published investigation of the conformational equilibrium of ^{13}C methyl phenyl sulfoxide,[62] a strong dependence of the conformational equilibrium has been observed going from cyanobicyclohexyl and cyanophenylcyclohexyl solvents (ZLI type solvents) to phenylbenzoates or benzylideneanilines (EBBA). On the other hand such effect has not been observed for ethylbenzene[63] (the shape of $U_{int}(\{\phi\})$ is quite insensitive to the solvents used, EBBA included), styrene,[52] or biphenyl (investigated in different solvents and using different models to decouple the internal and reorientational motions between, as summarized by Celebre et al.[21]). A fully unbiased investigation,[64−66] repeated with this much larger data set, could help in determining the real information content of the extra D_{HC} couplings and assessing the reliability of the AP results. Anyway, it is worth noticing that similar "solvent effects" have been observed also for 2-thiophencarboxaldehyde[58] (a narrower p^{ϕ} compared with DFT calculations but near the same p_{cis}/p_{trans} ratio) and for acrolein[53] (a significant lower population of the cis conformer compared with MW and theoretical studies), two cases recently reinvestigated with the same approach.

The effects of the force fields on the calculated value of internal geometrical parameters seem to be relatively small and smaller than the differences observed between the two solvents as reported in Table 7, this latter perhaps a consequence of having neglected in eq 1 the contribution of the vibration/orientation coupling[31,32] (but note that uncertainties in spectral analysis could not be ruled out, as discussed in section 2.1). Remembering that the covariance matrix elements are calculated using the normal modes, $w_{i\zeta}^{\nu}$, calculated at the theoretical minima as in eq 4 and that for 2,2′-bithiophene these are conspicuously different from the AP minima, it appears that the choice of the theoretical method used to calculate the force field is not so critical. The same conclusions could not apply for "rigid" molecules where internal parameters can be determined with higher precision and therefore the quality of the force field could play a more significant role.

Acknowledgment. This work has been supported by MIUR PRIN "Cristalli Liquidi e Macromolecole per Strutture Nanorganizzate". We thank Dr. F. Castiglione for her kindness and patience in recording the spectra

References and Notes

(1) Bäuerle, P. In *Electronic Materials: The Oligomer Approach*; Müllen, K.; Wegner, G., Eds.; Wiley: New York, 1998.
(2) Cornil, J.; Beljonne, D.; Brédas, J. In *Electronic Materials: The Oligomer Approach*; Müllen, K.; Wegner, G., Eds.; Wiley: New York, 1998.
(3) Fichou, D. *Simulation und automatisierte analyse von kernresonanzspektren*; Wiley-VCH: Weinheim, 1999.
(4) Ortí, E.; Viruela, P. M.; Sánchez-Marín, J.; Tomás, F. *J. Phys. Chem.* **1995**, *99*, 4955−4963.
(5) Grozema, F. C.; van Dujinen, P. T.; Berlin, Y. A.; Ratner, M. A.; Siebbeles, L. D. A. *J. Phys. Chem. B* **2002**, *106*, 7791−7795.
(6) Fichou, D. J. *J. Mater. Chem.* **2000**, *10*, 571−588.
(7) Marcon, V.; Raos, G. *J. Phys. Chem. B* **2004**, *108*, 18053−18064.
(8) César, N. D.; Belletête, M.; Leclerc, M.; Durocher, G. *Synth. Met.* **1998**, *94*, 291−298.
(9) Raos, G.; Famulari, A.; Marcon, V. *Chem. Phys. Lett.* **2003**, *379*, 364−372.
(10) Almenningen, A.; Bastiansen, O.; Svendsås, P. *Acta Chem. Scand.* **1958**, *12*, 1671−1674.
(11) Samdal, S.; Samuelsen, E. J.; Volden, H. V. *Synth Met.* **1993**, *59*, 259−265.
(12) Chadwick, J. E.; Kholer, B. E. *J. Phys. Chem.* **1994**, *98*, 3631−3637.
(13) Takayanagi, M.; Gejo, T.; Hanozaki, I. *J. Phys. Chem.* **1994**, *98*, 12893−12898.
(14) Visser, G. J.; Heeres, G. J.; Wolter, J.; Vos, A. *Acta Crystallogr. B* **1968**, *24*, 467−473.
(15) Lumbroso, H.; Carpanelli, C. *Bull. Soc. Chim. Fr* **1964**, 3198.
(16) Aroney, M. J.; Lee, H. K.; Le Fevre, R. J. W. *Aust. J. Chem.* **1972**, *25*, 1561−1564.
(17) Meunier, P.; Coustale, M.; Guimon, C.; Pfister-Guillouzo, G. J. *J. Mol. Struct.* **1977**, *36*, 233−242.
(18) Nordén, B.; Hakansson, R.; Sundbom, R. *Acta Chem. Scand.* **1972**, *26*, 429−433.
(19) Meunier, P.; Coustale, M.; Arian, J. *J. Bull. Soc. Chim Belg.* **1978**, *82*, 27−39.
(20) Orville-Thomas, W. J. *Internal Rotation in Molecules*; John Wiley & Sons: London, 1974.
(21) Celebre, G.; Longeri, M. NMR Studies of solutes in Liquid crystals: Small Flexible Molecules. In *NMR of Ordered Liquids*; Burnell, E. E., de Lange, C. A., Eds.; Kluwer: Dordrecht, The Netherlands, 2003.
(22) Emsley, J. W. Liquid Crystalline Samples: General Considerations. In *Encyclopedia of NMR*; Grant, D. M., Harris, R. K., Eds.; John Wiley & Sons: New York, 1996.
(23) Emsley, J. W. Liquid Crystalline Samples: Structure of Nonrigid Molecules. In *Encyclopedia of NMR*; Grant, D., Harris, R., Eds.; John Wiley & Sons: New York, 1996.
(24) Burnell, E. E.; de Lange, C. A. *NMR of Ordered Liquids*; Kluwer: Dordrecht, The Netherlands, 2003.
(25) Celebre, G.; De Luca, G.; Longeri, M.; Catalano, D.; Veracini, C. A.; Emsley, J. W. *J. Chem. Soc., Faraday Trans.* **1991**, *87*, 2623−2627.
(26) Bellitto, L.; Petrongolo, C.; Veracini, C. A.; Bambagiotti, M. *J. Chem. Soc., Perkin Trans. II* **1967**, 314−318.
(27) Ter Beek, L. C.; Zimmerman, D. S.; Burnell, E. E. *Mol. Phys.* **1991**, *74*, 1027−1035.
(28) Bucci, P.; Longeri, M.; Veracini, C. A.; Lunazzi, L. *J. Am. Chem. Soc.* **1974**, *96*, 1305−1309.
(29) Khetrapal, C. L.; Kunwar, A. C. *Mol. Phys.* **1974**, *28*, 441−446.
(30) Diehl, P. Structure of Rigid Molecules Dissolved in Liquid Crystalline Solvents. In *Encyclopedia of NMR*; Grant, D., Harris, R., Eds.; John Wiley and Sons: New York, 1996.
(31) Lounila, J.; Diehl, P. *Mol. Phys.* **1984**, *52*, 827−845.
(32) Lounila, J.; Diehl, P. *J. Magn. Reson.* **1984**, *56*, 254−261.
(33) Vivekanandan, S.; Suryaprakash, N. *Chem. Phys. Lett.* **2001**, *338*, 247−253.

(34) Emsley, J. W.; Merlet, D.; Smith, K. J.; Suryaprakash, N. *J. Magn. Reson.* **2002**, *154*, 303−310.
(35) Diehl, P. Molecular Structure from Dipolar Coulpling. In *NMR of Liquid Crystals*; Emsley, J., Ed.; Reidel: Dordrecht, The Netherlands, 1985.
(36) Emsley, J. W.; Luckhurst, G. R.; Stockley, C. P. *Proc. R. Soc. London A* **1982**, *381*, 117−138.
(37) Celebre, G.; De Luca, G.; Emsley, J. W.; Foord, E. K.; Longeri, M.; Lucchesini, F.; Pileio, G. *J. Chem. Phys.* **2003**, *118*, 6417−6426.
(38) Kalinowski, H. O.; Berger, S.; Braun, S. *Carbon-13 NMR Spectroscopy*; John Wiley & Sons: New York, 1988.
(39) Celebre, G.; De Luca, G.; Longeri, M.; Sicilia, E. *J. Chem. Inf. Comput. Sci.* **1994**, *34*, 539−545.
(40) Karpfen, A.; Choi, C. H.; Kertesz, M. *J. Phys. Chem. A* **1997**, *101*, 7426−7433.
(41) Duarte, H. A.; Santos, H. F. D.; Rocha, W. R.; Almeida, W. B. D. *J. Chem. Phys.* **2000**, *113*, 4206−4215.
(42) Wiberg, K. B. *J. Comput. Chem.* **2004**, *25*, 1342−1346.
(43) Scott, A. P.; Radom, L. *J. Phys. Chem.* **1996**, *100*, 16502−16513.
(44) Andersson, M. P.; Uvdal, P. *J. Phys. Chem. A* **2005**, *109*, 2937−2941.
(45) Frisch, M. J.; Trucks, G. W.; Schlegel, H. B.; Scuseria, G. E.; Robb, M. A.; Cheeseman, J. R.; Montgomery, J. A., Jr.; Vreven, T.; Kudin, K. N.; Burant, J. C.; Millam, J. M.; Iyengar, S. S.; Tomasi, J.; Barone, V.; Mennucci, B.; Cossi, M.; Scalmani, G.; Rega, N.; Petersson, G. A.; Nakatsuji, H.; Hada, M.; Ehara, M.; Toyota, K.; Fukuda, R.; Hasegawa, J.; Ishida, M.; Nakajima, T.; Honda, Y.; Kitao, O.; Nakai, H.; Klene, M.; Li, X.; Knox, J. E.; Hratchian, H. P.; Cross, J. B.; Bakken, V.; Adamo, C.; Jaramillo, J.; Gomperts, R.; Stratmann, R. E.; Yazyev, O.; Austin, A. J.; Cammi, R.; Pomelli, C.; Ochterski, J. W.; Ayala, P. Y.; Morokuma, K.; Voth, G. A.; Salvador, P.; Dannenberg, J. J.; Zakrzewski, V. G.; Dapprich, S.; Daniels, A. D.; Strain, M. C.; Farkas, O.; Malick, D. K.; Rabuck, A. D.; Raghavachari, K.; Foresman, J. B.; Ortiz, J. V.; Cui, Q.; Baboul, A. G.; Clifford, S.; Cioslowski, J.; Stefanov, B. B.; Liu, G.; Liashenko, A.; Piskorz, P.; Komaromi, I.; Martin, R. L.; Fox, D. J.; Keith, T.; Al-Laham, M. A.; Peng, C. Y.; Nanayakkara, A.; Challacombe, M.; Gill, P. M. W.; Johnson, B.; Chen, W.; Wong, M. W.; Gonzalez, C.; Pople, J. A. *Gaussian 03*, revision C.02; Gaussian, Inc.: Wallingford, CT, 2004.
(46) Schmidt, M. W.; Baldridge, K. K.; Boatz, J. A.; Elbert, S. T.; Gordon, M. S.; Jensen, J. H.; Koseki, S.; Matsunaga, N.; Nguyen, K. A.; Su, S. J.; Windus, T. L.; Dupuis, M.; Montgomery, J. A. *J. Comput. Chem.* **1993**, *14*, 1347−1363.
(47) Schaftenear, G. Copyright 1991.
(48) Zerbi, G.; Chierichetti, B.; Ingänas, O. *J. Chem. Phys.* **1991**, *94*, 4637−4645.
(49) Degli Esposti, A.; Zerbetto, F. *J. Phys. Chem. A* **1997**, *101*, 7283−7291.
(50) Wong, M. W. *Chem. Phys. Lett.* **1996**, *256*, 391−399.
(51) Barone, V. *J. Phys. Chem. A* **2004**, *108*, 4146−4150.
(52) Celebre, G.; De Luca, G.; Longeri, M.; Pileio, G.; Emsley, J. W. *J. Chem. Phys.* **2004**, *120*, 7075−7084.
(53) Celebre, G.; Concistré, M.; De Luca, G.; Longeri, M.; Pileio, G.; Emsley, J. W. *Chem. Eur. J.* **2005**, *11*, 3599−3608.
(54) Zannoni, C. Quantitative description of orientational order: rigid molecules. In *NMR of liquid crystals*; Emsley, J. W., Ed.; Reidel: Dordrecht, 1985.
(55) Diehl, P.; Jokisaari, J.; Amrein, J. *Org. Magn. Reson.* **1980**, *13*, 451−454.
(56) Emsley, J. W.; Horne, T. J.; Celebre, G.; De Luca, G.; Longeri, M. *J. Chem. Soc., Faraday Trans.* **1992**, *88*, 1679−1684.
(57) Inoue, K.; Takeuchi, H.; Konaka, S. *J. Phys. Chem. A* **2001**, *105*, 6711−6716.
(58) Concistré, M.; De Luca, G.; Longeri, M.; Pileio, G.; Emsley, J. W. *ChemPhysChem.* **2005**, *6*, 1483−1491.
(59) Lesot, P.; Merlet, D.; Courtieu, J.; Emsley, J. W.; Rantala, T. T.; Jokisaari, J. *J. Phys. Chem. A* **1997**, *101*, 5719−5724.
(60) Merlet, D.; Emsley, J. W.; Jokisaari, J.; Kaski, K. *Phys. Chem. Chem. Phys.* **2001**, *3*, 4918−4925.
(61) Pham, T. N.; Hinchley, S. L.; Rankin, D. W.; Liptaj, T.; Uhrin, D. *J. Am. Chem. Soc.* **2004**, *126*, 13100−13110.
(62) Celebre, G.; De Luca, G.; Maiorino, M.; Iemma, F.; Ferrarini, A.; Pieraccini, S.; Spada, G. P. *J. Am. Chem. Soc.* **2005**, *127*, 11736−11744.
(63) Algieri, C.; Castiglione, F.; Celebre, G.; De Luca, G.; Longeri, M.; Emsley, J. W. *Phys. Chem. Chem. Phys.* **2000**, *2*, 3405−3413.
(64) Di Bari, L.; Persico, M.; Veracini, C. A. *J. Chem. Phys.* **1992**, *96*, 4782−4791.
(65) Berardi, R.; Spinozzi, F.; Zannoni, C. *J. Chem. Soc., Faraday Trans.* **1992**, *88*, 1863−1873.
(66) Berardi, R.; Spinozzi, F.; Zannoni, C. *Liq. Cryst.* **1994**, *16*, 381−397.
(67) Irle, S.; Lischka, H. *J. Mol. Struct. (THEOCHEM)* **1996**, *364*, 15−31.
(68) Pulay, P.; Fogarasi, G.; Pang, F.; Boggs, J. *J. Am. Chem. Soc.* **1979**, *101*, 2550−2560.